https://doi.org/10.5194/essd-2026-547
Preprint. Discussion started: 5 August 2026

Open Access Earth System Science Data Discussions

AguaTrack-ARCO-SA: A 30-year, high-resolution atmospheric moisture tracking dataset for South America

Ho Tin Hung[1], Sung Che Lin[1], Kai-Chih Tseng[2], Wei Weng[3], and Li-Pen Wang[1, 4]

[1]Department of Civil Engineering, National Taiwan University, Taipei 10617, Taiwan
[2]Department of Atmospheric Sciences, National Taiwan University, Taipei 10617, Taiwan
[3]Department of Geography, National Taiwan University, Taipei 10617, Taiwan
[4]Department of Civil and Environmental Engineering, Imperial College London, London SW7 2AZ, UK

Correspondence: Ho Tin Hung (isaacgbhk@caece.net), Kai-Chih Tseng (kaichiht@ntu.edu.tw), Wei Weng (weiweng@ntu.edu.tw), and Li-Pen Wang (lpwang@ntu.edu.tw)

Abstract.

Atmospheric moisture recycling is a key component of the hydrological cycle, linking evapotranspiration to downwind precipitation. However, existing moisture tracking datasets are often limited by coarse spatial resolution, short temporal coverage, or high computational demands, constraining their use for subnational-scale and short-term event analyses. Here, we present AguaTrack-ARCO-SA, a 30-year (1990–2019), daily, 0.25° resolution atmospheric moisture backtracking dataset for South America, generated using the Eulerian WAM2layers v3 model driven by ERA5 reanalysis data. The dataset independently tracks moisture sources for approximately 25,000 land grid cells, providing detailed source–sink relationships at department to continental scales. The primary output variable, tracked evaporation, quantifies the contribution of each source grid cell to precipitation at each target location, alongside diagnostic variables for moisture gains, losses, and tagged precipitation. To facilitate efficient access, we compress the ∼230 TB of raw tracking output into an ∼8 TB Analysis-Ready, Cloud-Optimized (ARCO) product using Zarr storage. This structure enables scalable querying and analysis through cloud-based or local workflows without requiring high-performance computing resources. The dataset is openly available on Hugging Face (https://doi.org/10.57967/hf/8650) and the accompanying code and tutorials on GitHub (https://github.com/NTU-CompHydroMet-Lab/AguaTrack-ARCO-SA-Tutorial), supporting reproducibility and reuse. This dataset provides a high-resolution, long-term resource for analysing atmospheric moisture transport, precipitationsheds, and hydroclimatic variability across South America.

1 Introduction

Land-atmosphere interactions play a critical role in the hydrological cycle and are strongly coupled with regional climates (Seneviratne et al., 2006; Van Der Ent et al., 2010). A primary behaviour of this coupling is continental moisture recycling –a continuous process by which terrestrial evapotranspiration returns to the Earth's surface as downwind precipitation (Eltahir and Bras, 1996; Van Der Ent et al., 2014). As human activities (such as widespread deforestation, agricultural expansion, and irrigation) increasingly alter land surface fluxes, quantifying these atmospheric water flows has become critical for

https://doi.org/10.5194/essd-2026-547
Preprint. Discussion started: 5 August 2026

Open Access Earth System Science Data Discussions

anticipating shifts in regional water availability (Zemp et al., 2017; Wang-Erlandsson et al., 2018). To uncover these invisible atmospheric pathways, moisture tracking has been widely adopted in modern hydroclimatology (Kalverla et al., 2025). This technique allows researchers to delineate *precipitationsheds*, the specific upwind oceanic and terrestrial regions that supply evaporation to a downwind location's rainfall (Keys et al., 2012, 2014). Applying this concept reveals how geographically remote ecosystems and human societies are inextricably linked, demonstrating that localised land management can exert remote impacts on regional water security (Keys et al., 2018, 2024; Posada-Marín et al., 2024).

To explicitly map and quantify these intricate source-sink relationships, Eulerian numerical moisture tracking models, specifically the Water Accounting Model-2layers (WAM2layers), have been extensively utilised across diverse global and regional applications (Guo et al., 2019; Tuinenburg et al., 2020; Shi et al., 2022; Kalverla et al., 2025). Operating directly on fixed geographic grids driven by atmospheric reanalysis data, WAM2layers traces the flow of tagged moisture by strictly closing the atmospheric water budget at every time step (Kalverla et al., 2025). By conceptualising the atmospheric column into two vertical layers, the framework estimates vertical moisture exchange, ensuring a physically robust representation of atmospheric moisture transport (Zhang, 2020; Chen et al., 2023). Because this Eulerian approach diagnoses evaporation and precipitation fluxes directly on the grid and continuously adheres to the regional mass balance, it has been deployed to investigate the atmospheric drivers of severe droughts, extreme precipitation events, and remote moisture feedbacks (Benedict et al., 2020; Zhang et al., 2023; Mu et al., 2021). The recent development of WAM2layers v3 (Kalverla et al., 2025) further optimises this fundamental approach, providing the immense computational efficiency required to ingest decades of high-resolution ERA5 data across massive continental domains.

South America serves as a premier domain for applying atmospheric moisture tracking models due to its diverse hydroclimate and profoundly uneven spatial distribution of water resources. The continent encompasses some of the most extreme precipitation gradients on Earth, ranging from the hyper-arid Atacama Desert to the hyper-humid Pacific coast of Colombia and the massive tropical expanses of the Amazon basin (Enciso et al., 2022; Lobos-Roco et al., 2022; Ampuero et al., 2020; Zemp et al., 2017, 2014). As a result of this complex climatology, the region is highly susceptible to severe hydroclimatic extremes, frequently oscillating between devastating basin-wide floods and intensifying multi-year droughts that threaten urban water security, hydropower generation, and agricultural productivity (Mu et al., 2021; Posada-Marín et al., 2024; Boisier et al., 2025; Garreaud et al., 2025; Weng et al., 2020; Magrin et al., 2014; Tian et al., 2016). Governing this volatile distribution of water resources is a deeply interconnected continental atmospheric network. The Amazon rainforest acts as a massive terrestrial "water pump," evaporating vast quantities of moisture that prevailing winds, the "Aerial River", transport westward against the steep topographic barrier of the Andes, which then channel the moisture southward into the highly populated and agriculturally vital La Plata basin (Arraut et al., 2012; Zemp et al., 2014; Ampuero et al., 2020; Weng et al., 2018). This transcontinental transport drives a remote moisture recycling effect, establishing complex precipitationsheds where evaporation from one distinct ecological zone sustains the rainfall of another (Keys et al., 2012, 2014). Because of this deep spatial connectivity, localised land activities, such as rapid deforestation or large-scale agricultural expansion, act as multipliers on regional hydrology. They are capable of triggering profound hydroclimatic

https://doi.org/10.5194/essd-2026-547
Preprint. Discussion started: 5 August 2026

Open Access Earth System Science Data Discussions

disruptions that exacerbate drought conditions and threaten ecosystem resilience thousands of kilometres downwind (Erfanian et al., 2017; Wang-Erlandsson et al., 2018; Mu et al., 2023).

Despite the critical need to understand these atmospheric teleconnections, current open-source moisture tracking datasets often lack the spatio-temporal granularity required for multi-scale analysis in South America. While pioneering global datasets provide foundational insights into moisture recycling networks (Tuinenburg and Staal, 2020; Link et al., 2020), their immense computational demands often necessitate heavy data aggregation. Consequently, these products frequently provide data at monthly timescales or spatial resolutions exceeding 1.0° (Berger et al., 2025; Zan et al., 2024), while lumping moisture sinks into coarse grids. This spatial and temporal coarsening process obscures the regional, daily weather extremes, such as flash droughts and rapid-onset intense storm systems, that dictate regional water security, leaving a significant literature gap for localised environmental, ecological, and agricultural research.

To bridge this critical gap, we present a novel, open-access dataset designed to directly overcome these existing limitations through three core contributions. First, to capture both long-term climatology and daily weather extremes, we introduce a 30-year, high-resolution (0.25°, daily) atmospheric moisture backtrack dataset specifically tailored to the South American continent (tracking domain: 90°W–25°W, 60°S–15°N). Second, to resolve the issue of coarse spatial lumping, we implement a "finest tagging area" methodology, independently tracking the evaporative sources for ∼25,000 individual 0.25° land grid cells. This high-density grid empowers users to perform seamless, bottom-up spatial aggregations, scaling from local departments to trans-boundary basins. Finally, the immense computational cost and hardware barriers associated with running these models and manipulating a 230 TB+ tracking dataset typically prevent researchers and water managers, particularly those in developing countries, from utilising such advanced tools. To explicitly solve this bottleneck, we engineered this product using an Analysis-Ready, Cloud-Optimized (ARCO) architecture. Paired with comprehensive, open-source coding tutorials, this infrastructure democratises access to Earth system big data. It allows researchers and decision-makers to efficiently query and visualise decades of high-resolution atmospheric flows without the prohibitive need for localised high-performance computing clusters.

2 Material and methods

2.1 Moisture Tracking Model (WAM2layers v3)

The dataset was generated using the recently updated Water Accounting Model-2layers (WAM2layers v3) (Kalverla et al., 2025), a highly efficient Eulerian moisture tracking model. WAM2layers solves a prognostic atmospheric water balance equation over a fixed geographic grid. To adequately account for vertical moisture exchange where moisture may be transported in different directions at different altitudes, the model compresses the atmospheric column into two functional layers (an upper and a lower layer). The governing moisture mass balance is defined as:

$$\frac{\Delta_t S}{\Delta t} + \frac{1}{A}(\Delta_x F_x + \Delta_y F_y + \Delta_p F_p) = E - P \tag{1}$$

where S represents the atmospheric moisture storage (precipitable water), t is time, A is Area, F_x and F_y are the zonal and meridional moisture fluxes, E is evaporation entering the layer, P is precipitation removed from the atmosphere, and F_p represents the vertical moisture exchange driven by vertical wind velocity and turbulence (Kalverla et al., 2025).

For the purposes of this dataset, WAM2layers was configured in backtracking (receptor-oriented) mode. In this configuration, precipitation (P) falling within a specified target grid cell is labelled as "tagged precip." As the model steps backward in time, it advects this tagged water through the two atmospheric layers using reversed wind fields, systematically allocating the moisture back to the geographic locations and specific quantities of surface evaporation (E) that originally supplied the precipitation event.

2.2 Atmospheric Forcing Data and Preprocessing

To drive the Eulerian water balance described above, WAM2layers requires continuous, physically consistent atmospheric boundary conditions. We utilised historical atmospheric data from the fifth-generation European Centre for Medium-Range Weather Forecasts (ECMWF) atmospheric reanalysis (ERA5) (Hersbach et al., 2020; Carver and Merose, 2023). ERA5 offers an improved representation of the global hydrological cycle relative to earlier reanalysis products and is now widely used for atmospheric moisture tracking.

For the data preprocessing, we downloaded single-level variables, including total precipitation (`tp`), evaporation (`e`), surface pressure (`sp`), and total column water (`tcw`), alongside multi-level variables such as specific humidity (`q`) and the eastward (`u`) and northward (`v`) wind components. To capture the vertical profile necessary for the two-layer separation, the multi-level variables were extracted on 22 specific terrain-following model levels. During preprocessing, ERA5 data were spatially cropped to our predefined South American tracking domain (90°W–25°W, 60°S–15°N). Specifically, all ERA5 input data were obtained at a 1-h temporal resolution at their native $0.25° \times 0.25°$ spatial grid (Table 1). This represents a substantial advancement in spatial and temporal granularity compared to previous continental tracking efforts, allowing for a vastly improved representation of complex topographical influences, such as the Andes mountains, and the diurnal convective cycles of the Amazon basin.

2.2.1 Mass Conservation and Vertical Integration

Since the core tracking algorithm of WAM2layers operates on two functional vertical layers (an upper and a lower layer), its built-in pre-processing module must first rigorously integrate the complex 3D atmospheric input to ensure strict mass conservation. Specifically, the WAM2layers pre-processor ingests 3D atmospheric variables across a selected subset of 22 ERA5 vertical model levels (see Table 1). To compress this high-resolution vertical structure into two layers without violating the regional water balance, the specific humidity (`q`) across all 22 input levels is first vertically integrated to compute the preliminary column water vapour. This integrated value is then scaled by a dynamic correction factor to exactly match the 2D total column water (`tcw`) provided directly by the single-level ERA5 surface level dataset. Once scaled, the corrected moisture and wind fields are aggregated into their respective upper and lower layers. By explicitly forcing the vertically integrated moisture field to align with the 2D total column water, this WAM2layers pre-processing step guarantees strict closure of the

https://doi.org/10.5194/essd-2026-547
Preprint. Discussion started: 5 August 2026

Open Access Earth System Science Data Discussions

Table 1. Summary of ERA5 atmospheric forcing variables utilised to drive the WAM2layers v3 model.

Variable Name	**Short Name**	**Type / Model Level**	**Usage in WAM2layers**
Total precipitation	`tp`	Surface level	Prescribes the moisture sink removed from the atmosphere.
Evaporation	`e`		Prescribes the moisture source entering the lower atmospheric layer.
Surface pressure	`sp`		Computes exact model level pressures and the two-layer separation boundary.
Total column water	`tcw`		Corrects the vertically integrated specific humidity to close the water budget.
Specific humidity	`q`	**Upper layer:** 20, 40, 60, 80, 90, 95, 100, 105, 110 **Lower layer:** 115, 120, 123, 125, 128, 130, 131, 132, 133, 134, 135, 136, 137	Provides the specific humidity field required to quantify atmospheric moisture mass and calculate moisture storage over time.
Wind components	`u`, `v`		Drives the advection scheme by providing zonal and meridional velocities, dictating the direction and magnitude of horizontal moisture transport fluxes.

Note: All variables have a temporal resolution of 1-Hourly and a spatial resolution of $0.25° \times 0.25°$.

water budget before the actual tracking begins, a procedure critical for minimising the accumulation of numerical moisture loss over a continuous 30-year simulation.

2.3 Tracking Execution and Parameters

To maintain the integrity of the Eulerian grid and avoid numerical instability, the tracking time step should satisfy the Courant–Friedrichs–Lewy (CFL) condition (Kalverla et al., 2025). This condition dictates that moisture fluxes must not completely cross a grid cell within a single computational timestep. To ensure stability, the ERA5 forcing data were linearly interpolated to a tracking timestep of 10 min. This high-frequency integration ensures that moisture fluxes moving rapidly across the $0.25°$ grid boundaries are captured without computational loss.

Furthermore, a critical consideration in backward moisture tracking is the atmospheric residence time of water vapor. Moisture evaporated from a source region may travel through the atmosphere from 8 to 10 days before precipitating over a target region (Van Der Ent and Tuinenburg, 2017; Van Der Ent et al., 2014). To account for this time lag, we implemented a 30-day "prewarming" (or spin-up) period. For example, to accurately map the evaporative sources of precipitation occurring in January 2019, the backward tracking process continuously ran backward through December 2018. Over this 1-month traceback duration, more than 95% of the tagged precipitation moisture is successfully allocated to its original surface evaporative sources, leaving a negligible fraction of "untracked" atmospheric moisture at the end of the simulation (Van Der Ent and Tuinenburg, 2017).

2.4 High-Resolution Tagging Strategy and Data Structure

The most computationally demanding and unique aspect of this dataset is the parallelised tagging strategy. Instead of defining large, predefined macro-regions (e.g., tracking moisture for the entire Amazon basin simultaneously), we treated every single 0.25° land grid cell across the South American continent (approximately 25,000 independent cells) as a fully separate precipitation sink (receptor).

While treating ∼25,000 grids as independent receptors provides unparalleled spatial flexibility for end-users, it inherently results in an exceptionally dense data structure. The output of this tracking strategy is a four-dimensional array with the axes: `[time, source_latitude, source_longitude, tagging_mask]`. For 30 years of daily tracking across the continent, this 4D tensor inflates to over 230 Terabytes of raw output data. However, because the tracking is resolved down to this "finest possible tagging area," users are no longer restricted by predefined boundaries set by the dataset creators. Users can query the `tagging_mask` axis to isolate individual department-scale agricultural townships, or aggregate thousands of receptors to evaluate transboundary river basins. To make querying a dataset of this magnitude feasible for the broader scientific community, the raw output was subsequently transformed into an Analysis-Ready, Cloud-Optimized (ARCO) architecture, detailed in Sect. 3.3.

3 Results

3.1 Data Variables and Dimensions

The resulting dataset contains a comprehensive suite of moisture tracking variables resolved at daily intervals for the entire 30-year period (1990–2019). The primary output variable is *tracked evaporation* (`e_track`), which represents the explicit volume of evaporation from any source grid cell within the tracking area that eventually contributed to precipitation in the target receptor grids. The data variables are stored in a multi-dimensional array spanning time, the target receptor index (`tagging_mask`), and the source `latitude` and `longitude`. Each `tagging_mask` index corresponds to one tagged 0.25° land cell, whose geographic position is given by the accompanying `tag_lat` and `tag_lon` coordinate arrays; a user therefore maps a city or basin to its receptor index by a nearest-neighbour search over (`tag_lat`, `tag_lon`). Note that the `latitude` coordinate is stored in descending order (from $+15°$ to $-60°$). Additional diagnostic variables, including moisture `gains`, `losses`, and `tagged_precip`, are also provided to allow for complete regional water balance assessments (see Table 2).

https://doi.org/10.5194/essd-2026-547
Preprint. Discussion started: 5 August 2026

Table 2. Dataset Variables and Dimensions. A comprehensive list of the data variables provided in the primary dataset, including their descriptions, units, and array shapes.

Variable	Description	Units	Dimensions (Shape)
`e_track`	Tracked evaporation that will end up as tagged precipitation	mm day^{-1}	`(time, tagging_mask, latitude, longitude)`
`gains`	Moisture gained during the tracking	mm day^{-1}	`(time, tagging_mask, latitude, longitude)`
`losses`	Moisture lost during the tracking	mm day^{-1}	`(time, tagging_mask, latitude, longitude)`
`tagged_precip`	Precipitation falling on the tagged receptor	mm day^{-1}	`(time, tagging_mask)`

Note: Values are per-day accumulations. Spatial resolution for source coordinates is 0.25° × 0.25°; temporal resolution is daily.
Array dimensions per annual file: `time` = 365/366, `tagging_mask` = 25,186, `latitude` = 301, `longitude` = 261.

3.2 Tracking Stability and Mass Conservation

As a commitment to data transparency and to satisfy rigorous quality control standards, tracking stability and debug metrics generated by WAM2layers are included alongside the main dataset. Because Eulerian tracking requires strict numerical stability, supplementary debug files are provided in NetCDF (`.nc`) format. These debug files record the specific correction factors applied whenever numerical limits, such as the Courant–Friedrichs–Lewy (CFL) criterion, are reached (i.e., when the model time step is not sufficiently small for the local wind speed).

Specifically, these debug logs are saved when boundary limits are triggered to enforce mass conservation: the first limit ensures that the combined meridional and zonal fluxes can at most empty the grid cell, preventing the creation of any artificial numerical water gains. The second limit guarantees that the gross vertical flux also cannot exceed the total moisture available to empty the grid cell (Kalverla et al., 2025). Continuous evaluation of these stability metrics demonstrates that unexplained water loss errors (e.g., moisture lost due to numerical dispersion or domain boundary crossings) are limited to approximately 0.002% across the 30-year period. This confirms that the tracking maintained strict numerical mass conservation across the 30-year simulation, with only a negligible residual water-balance error.

3.3 Analysis-Ready, Cloud-Optimized (ARCO) Architecture

Given that the raw output of independently tracking ∼25,000 grids over 30 years totals roughly 230 Terabytes, traditional flat-file data distribution (e.g., distributing thousands of standard NetCDF files) would severely hinder data accessibility and usability. To democratise access to this massive hydroclimatic resource, we structured the dataset using an Analysis-Ready, Cloud-Optimized (ARCO) architecture based on the Zarr storage format, which compresses the archive to approximately 8 TB.

https://doi.org/10.5194/essd-2026-547
Preprint. Discussion started: 5 August 2026

This ARCO structure employs an advanced chunking strategy optimised for rapid spatio-temporal querying. By chunking the data strategically along the `tagging_mask` dimension while preserving the full length of the temporal and spatial dimensions within each chunk (chunk shape ≈ (365, 10, 301, 261), stored as Zarr v3 with blosc/zstd compression), users leveraging lazy-loading libraries (such as Xarray in Python) can extract a 30-year temporal profile for a single micro-basin or generate a single-day spatial map across the entire continent. This cloud-native architecture allows users to perform computations directly in the cloud and download only the specific megabytes of data they actually need, bypassing the requirement for local High-Performance Computing (HPC) clusters. In addition to the native daily store, we provide calendar-month and calendar-year aggregates (summed `e_track` and `tagged_precip`, together with an explicit land–sea mask `lsm`) as separate consolidated Zarr stores for analyses that do not require daily resolution.

3.4 Comparison with Existing Literature

To benchmark the physical consistency of our dataset and demonstrate the profound value of its fine spatial granularity, we compared our aggregated continental statistics against established datasets. Specifically, because our record spans 30 years, we averaged our 0.25° output over the common 2001–2018 period covered by the baseline estimates — the WAM2layers v2 dataset (Link et al., 2020) and the 3D Quasi-Isentropic Back-Trajectory (3DQIBT) method (Dirmeyer et al., 2009), as compiled and reported by Link et al. (2020) — so that all datasets are compared over an identical period.

We first compared the mean Terrestrial Evaporative Source (TES, defined as the fraction of precipitation that originated as evaporation from terrestrial sources by Dirmeyer et al. (2009)) and Country Internal Evaporative Source (CIES, defined as the fraction of precipitation that originated as evaporation from within the same country by Dirmeyer et al. (2009)) over major South American countries. As detailed in Table 3, the macro-scale evaporative source fractions derived from our dataset exhibit strong spatial pattern consistency with the baseline estimates reported by Link et al. (2020). For example, all models correctly identify Brazil as having the highest reliance on internal precipitation sources (CIES) due to its massive land area, while landlocked nations such as Paraguay and Bolivia exhibit the highest overall dependence on terrestrial moisture recycling (TES).

Notably, for the majority of countries our 0.25° dataset produces lower (more conservative) source fractions than the coarser models (e.g., Brazil TES: 30.9% compared to 36.7% in WAM2layers v2 and 56.7% in the 3D QIBT estimates); a minority of cases (e.g., Ecuador and Peru TES, and several CIES values) instead show slightly higher fractions, consistent with the bidirectional nature of the resolution-induced offset described below. The spatial distribution of these differences is illustrated in Fig. 1. These variations highlight the inherent advantage of utilising high-resolution atmospheric forcing. Coarse atmospheric data (such as 1.5° grids) are inherently susceptible to numerical diffusion. While conventional tracking studies apply land-sea masks to mitigate this, the sheer size of coarse grids inevitably blurs sharp coastal boundaries, acting as a bidirectional offset that can either artificially inflate or arbitrarily reduce terrestrial mixing depending on how the grid aligns with the mask (Li et al., 2024). This resolution-induced variance is especially pronounced in smaller or geographically narrow countries, such as Chile, where a single coarse grid cell may simultaneously straddle the open ocean, the coastline, and the steep topography of

https://doi.org/10.5194/essd-2026-547
Preprint. Discussion started: 5 August 2026

the Andes. By adequately resolving these fine-scale spatial gradients, the hourly, $0.25°$ ERA5 forcing data effectively curtails these numerical artifacts, resulting in a more constrained and physically realistic representation of continental water balances.

The primary advantage of this new dataset emerges most clearly at the regional and sub-regional scales, where spatial resolution becomes the limiting factor in assessing topographically complex domains. While coarse datasets adequately capture bulk continental averages, their large spatial granularity limits the refinement of regional variations. As shown in Fig. 2, a spatial comparison of the 2001–2018 average precipitationshed for the La Plata basin reveals stark differences between the datasets. Our $0.25°$ dataset provides a much-needed spatial refinement, better aligning with the sharp topographic boundary of the Andes Mountains. In contrast, the massive grid cells of the $1.5°$ WAM2layers v2 data (Link et al., 2020) inevitably blur these physical boundaries. While no reanalysis data can perfectly resolve the complex microphysics of mountain atmospheric interactions, the critical advantage of the $0.25°$ resolution lies in spatial representation. Finer-scale geographic features, most notably the exceptionally narrow terrestrial extent of Chile along the western coastline, are frequently subsumed by single grid cells in coarse models, merging ocean, coast, and mountain into one data point. By explicitly resolving these narrow coastal geometries, the $0.25°$ dataset allows for localised moisture attribution that is geometrically difficult at the $1.5°$ scale.

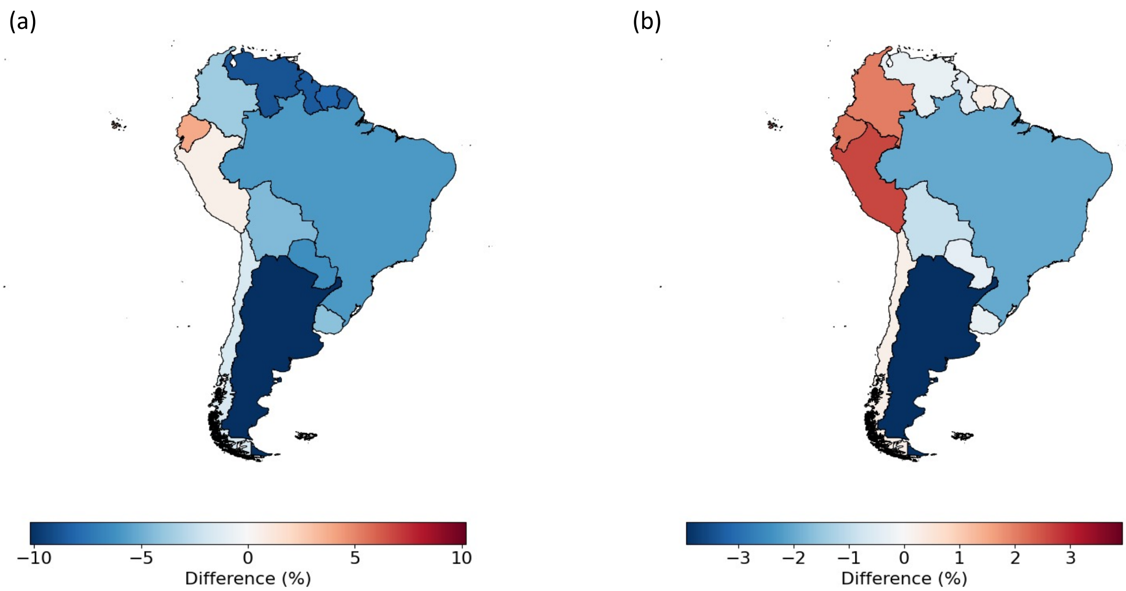

Figure 1. Spatial distribution of the differences between our high-resolution $(0.25°)$ dataset and the coarser $(1.5°)$ WAM2layers v2 baseline. Differences are calculated as WAM2layers v3 minus WAM2layers v2 for (a) Terrestrial Evaporative Source (TES) and (b) Country Internal Evaporative Source (CIES).

https://doi.org/10.5194/essd-2026-547
Preprint. Discussion started: 5 August 2026

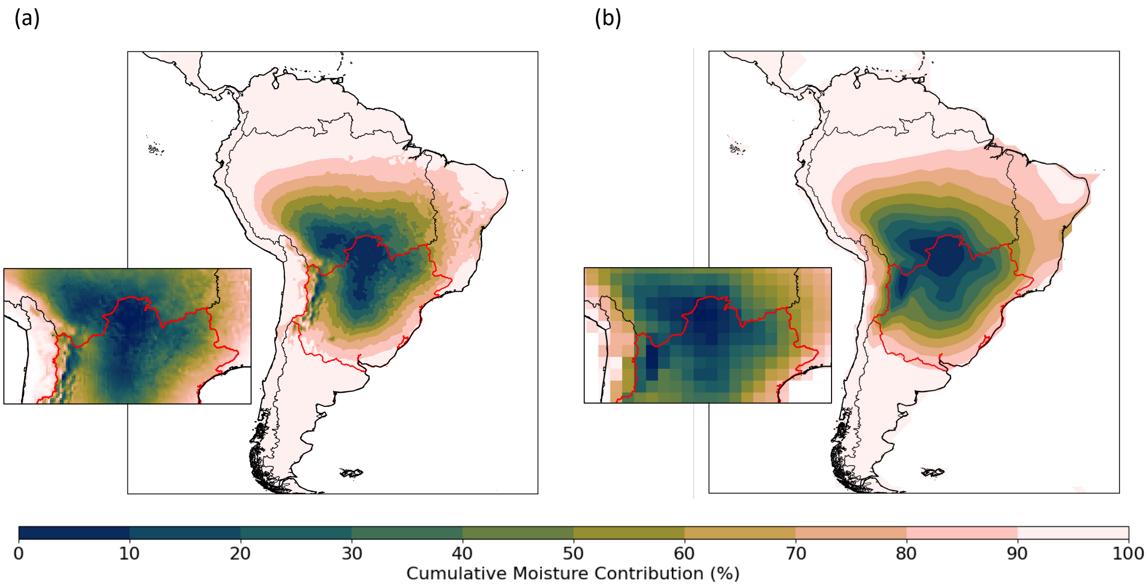

Figure 2. Comparison of the continental precipitationshed for the La Plata basin (2001–2018 average). (a) The 0.25° dataset explicitly resolves the topographical blocking effect of the Andes Mountains on moisture transport, whereas (b) the coarser 1.5° WAM2layers v2 dataset (Link et al., 2020) artificially smooths and blurs this critical climatic boundary.

4 Discussion

4.1 Usage Showcase

To demonstrate the scientific value and analytical flexibility of the new 30-year (1990–2019), daily, 0.25° resolution WAM2layers moisture backtrack dataset, we present five illustrative applications. These examples illustrate how the dataset's unprecedented spatial and temporal granularity can be leveraged to address diverse, pressing eco-hydrological and climatological questions across South America.

4.1.1 Intra-annual Seasonality and the South American Low-Level Jet

The South American Monsoon System and the South American Low-Level Jet (SALLJ) drive intense seasonal redistributions of atmospheric moisture across the continent (Marengo et al., 2004; Garreaud, 2009; Espinoza Villar et al., 2009). Using the dataset's monthly aggregated trajectories across all twelve calendar months of 2019, researchers can visualise how moisture sources expand and contract intra-annually (Fig. 3). For instance, focusing on a single 0.25° receptor grid over Viedma in northern Patagonia (63.00°W, 40.75°S), the data reveals the seasonal footprint of the South American Low-Level Jet (SALLJ). During the austral autumn and early winter (April to June), a distinct continental moisture corridor extends northward into

https://doi.org/10.5194/essd-2026-547
Preprint. Discussion started: 5 August 2026

Open Access Earth System Science Data Discussions

Table 3. Inter-comparison of mean Terrestrial Evaporative Source (TES) and Country Internal Evaporative Source (CIES) across South American countries, all averaged over the common 2001–2018 period. The comparison highlights the differences between our high-resolution (0.25°) dataset, the older WAM2layers v2 dataset (1.5°; Link et al. 2020), and a 3D QIBT model (Dirmeyer et al., 2009) as reported by Link et al. (2020).

	Terrestrial Evaporative Source (TES, %)			Country Internal Evap. Source (CIES, %)		
Country	**This Dataset**	**WAM2layers v2**	**3D QIBT**	**This Dataset**	**WAM2layers v2**	**3D QIBT**
Argentina	40.4	50.6	59.5	15.1	19.0	27.9
Bolivia	54.9	59.4	82.7	15.0	16.0	24.2
Brazil	30.9	36.7	56.7	26.9	28.9	46.3
Chile	2.7	4.3	8.1	1.6	1.4	5.4
Colombia	33.5	37.1	49.9	13.6	11.6	10.9
Ecuador	42.4	38.5	62.7	9.7	7.6	4.9
French Guiana	3.4	12.0	14.5	2.3	2.3	2.6
Guyana	7.8	16.4	19.1	2.8	3.2	3.2
Paraguay	55.5	61.9	90.0	6.1	6.5	13.0
Peru	49.8	49.2	71.8	19.1	16.5	25.9
Suriname	6.7	14.8	18.2	3.3	3.0	2.8
Uruguay	51.1	55.3	75.1	2.5	2.8	8.1
Venezuela	18.2	27.0	29.4	9.5	9.8	9.1

the Amazon basin, explicitly capturing how the SALLJ channels equatorial moisture poleward to feed semi-arid Patagonian environments (Salio et al., 2007).

4.1.2 Tracking Moisture Origins of Synoptic Extreme Events

Heavy rainfall and deadly landslides frequently devastate the steep coastal topography of southeastern Brazil, largely driven by the South Atlantic Convergence Zone (SACZ) and localised convective triggering (Carvalho et al., 2004; Seluchi et al., 2011). By utilising the dataset's daily temporal resolution, researchers can track the precise oceanic and terrestrial moisture sources feeding fast-moving, extreme synoptic events, such as the catastrophic rainfall that struck the Serra do Mar region in January 2011 (Fig. 4). Because the dataset avoids the smoothing effect of monthly averages, users can isolate the exact days of extreme precipitation (e.g., January 11 to 16, peaking at 30.7 kg m^{-2} day^{-1}) and calculate backward trajectories to differentiate the advective contributions of the SALLJ versus direct Atlantic oceanic influx during the event's lifecycle.

https://doi.org/10.5194/essd-2026-547
Preprint. Discussion started: 5 August 2026

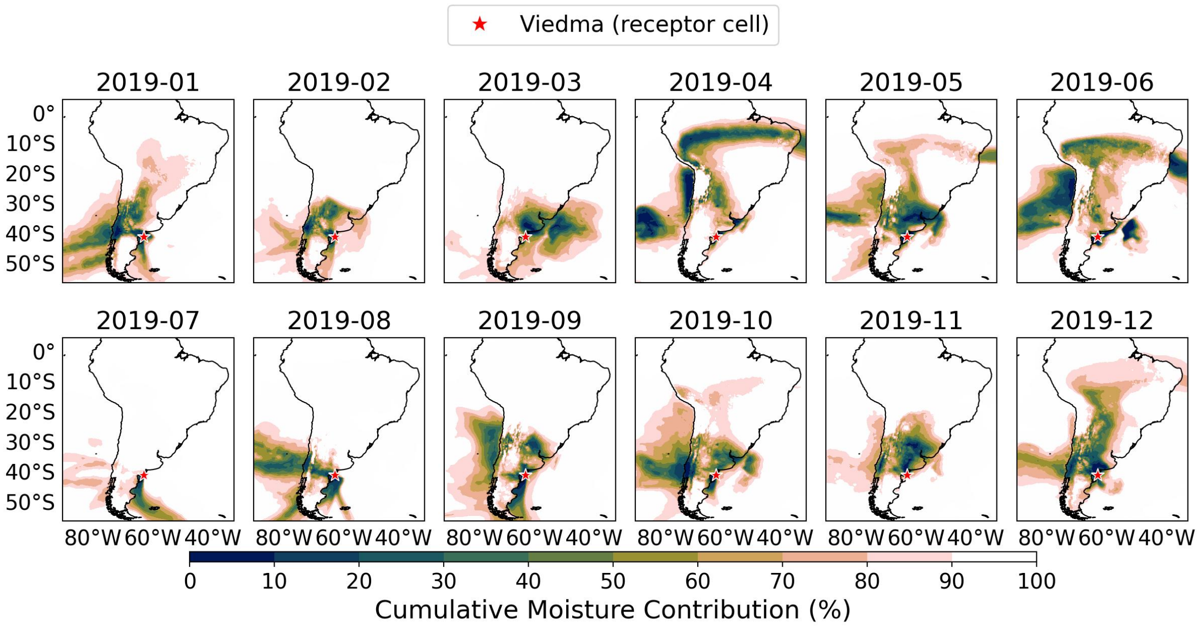

Figure 3. Monthly evolution of the precipitationshed for a 0.25° target grid over Viedma, Patagonia (63.00°W, 40.75°S; red star), during 2019. Each panel is a per-panel spatial cumulative distribution of the tracked-evaporation source field, ranked so that 0% marks the single strongest source cell and 100% the diffuse tail.

4.1.3 Multi-Decadal Anomalies During the Central Chile Megadrought

Since 2010, central Chile (30°S–40°S) has experienced an uninterrupted sequence of dry years, widely known as the "Megadrought," driven by a combination of natural oceanic forcing and anthropogenic climate change (Boisier et al., 2016; Garreaud et al., 2017). Leveraging the continuous 30-year span of this dataset, the megadrought can be characterised as a departure from the full-record (1990–2019) climatological precipitationshed (Fig. 5a). Whereas the 1990–2009 baseline sits slightly above the long-term mean, the 2010–2019 drought decade exhibits a coherent below-normal moisture-source anomaly concentrated around the central-Chile receptor. Partitioning the annual supply into continental and oceanic components (Fig. 5b) shows that the Pacific Ocean dominates the budget throughout, and that the continental recycling ratio remains essentially unchanged (∼28%) between the two periods, indicating that the drought reflects a reduction in the total moisture supply rather than a shift in the balance between oceanic advection and continental recycling.

4.1.4 High-Resolution Precipitationsheds and Continental Aerial Rivers

Deforestation in the Amazon basin threatens the stability of "aerial rivers" that supply precipitation to downwind, moisture-dependent regions (Zemp et al., 2014; Weng et al., 2019). Thanks to the ultra-fine 0.25° tagging of this dataset, users are not restricted to large, pre-defined river basins; any single 0.25° grid cell can be treated as a localised target sink and its

https://doi.org/10.5194/essd-2026-547
Preprint. Discussion started: 5 August 2026

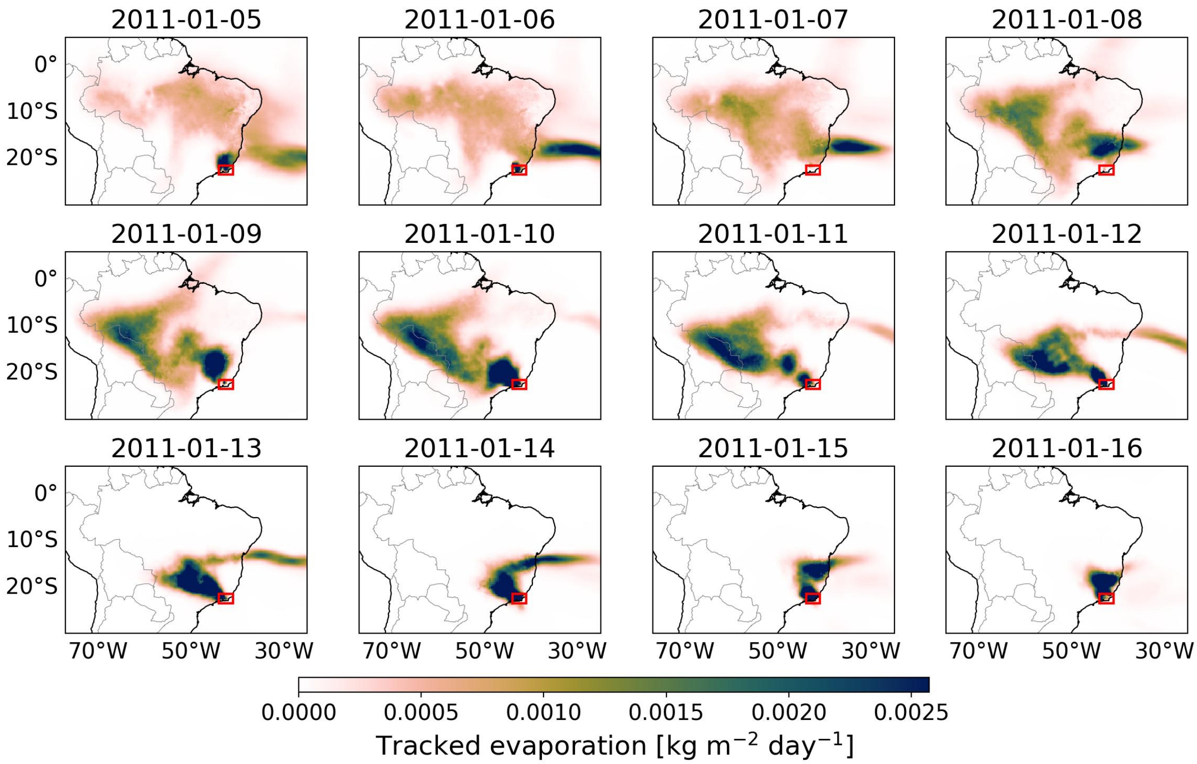

Figure 4. Daily evolution and spatial origins of moisture feeding the extreme precipitation event in the Serra do Mar region, Brazil (January 5–16, 2011). Each panel shows the precipitation- and area-weighted daily tracked-evaporation source field; the red box marks the Serra do Mar receptor region.

full 30-year climatological precipitationshed reconstructed. Figure 6 contrasts the 1990–2019 mean precipitationsheds of six such receptor cells spanning distinct climate regimes: the Amazon-fed sinks — Manaus, Santa Cruz de la Sierra, and São Paulo — expose the continental aerial rivers of Amazonian evapotranspiration that sustain downwind rainfall, whereas the Pacific-facing sink of Santiago draws almost entirely on oceanic, westerly-transported moisture, and the eastern-slope sinks of Buenos Aires and Viedma depend on the continental La Plata/SALLJ corridor — with Viedma receiving a more mixed continental, Atlantic, and trans-Andean Pacific supply. This high-resolution traceability provides the necessary foundation for evaluating urban water security (Keys et al., 2018) and designing targeted, cross-border forest conservation strategies.

4.1.5 ENSO-Driven Interannual Variability in Central-South Chile

The El Niño-Southern Oscillation (ENSO) is a dominant driver of interannual hydroclimatic variability in South America, particularly altering the position and intensity of extratropical storm tracks making landfall in Chile (Cai et al., 2020; Montecinos and Aceituno, 2003). By compositing the four seasons of the 1997/98 El Niño (JJA 1997 through MAM 1998) against those of the subsequent 1998/99 La Niña (JJA 1998 through MAM 1999), the dataset illustrates drastic shifts in

https://doi.org/10.5194/essd-2026-547
Preprint. Discussion started: 5 August 2026

Open Access Earth System Science Data Discussions

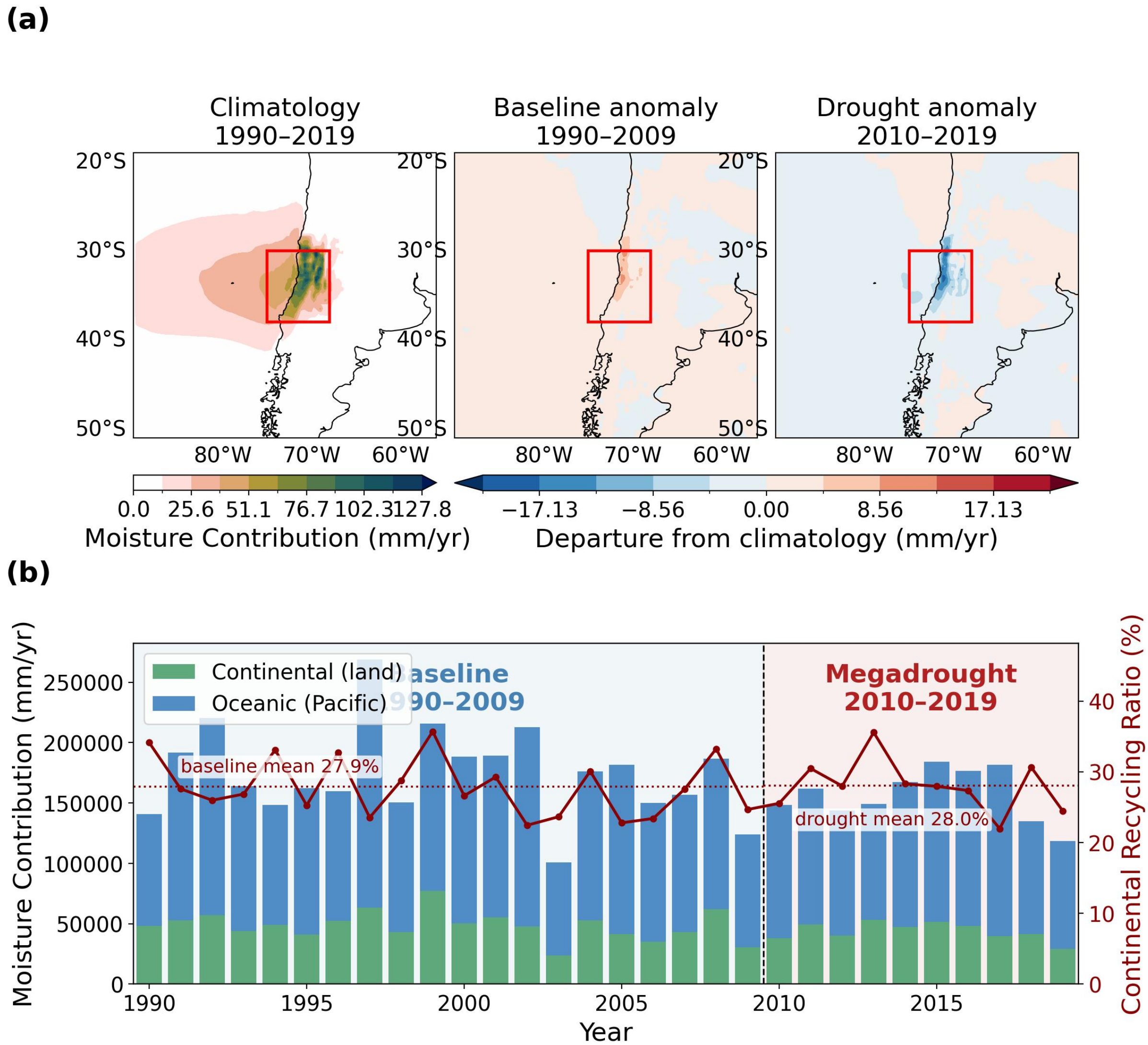

Figure 5. Climatological moisture sources of a central-Chile receptor box (red box) and their megadrought departure. (a) The 30-year mean precipitationshed (1990–2019; left), and the departures of the historical baseline (1990–2009; middle) and the megadrought decade (2010–2019; right) from that climatology, where blue denotes a below-normal moisture source. (b) Annual moisture supply partitioned into continental (land, green) and oceanic (Pacific, blue) sources (stacked bars, mm yr^{-1}), overlaid with the interannual continental recycling ratio (dark-red line); dotted lines mark the baseline and drought-period means.

https://doi.org/10.5194/essd-2026-547
Preprint. Discussion started: 5 August 2026

Open Access Earth System Science Data Discussions

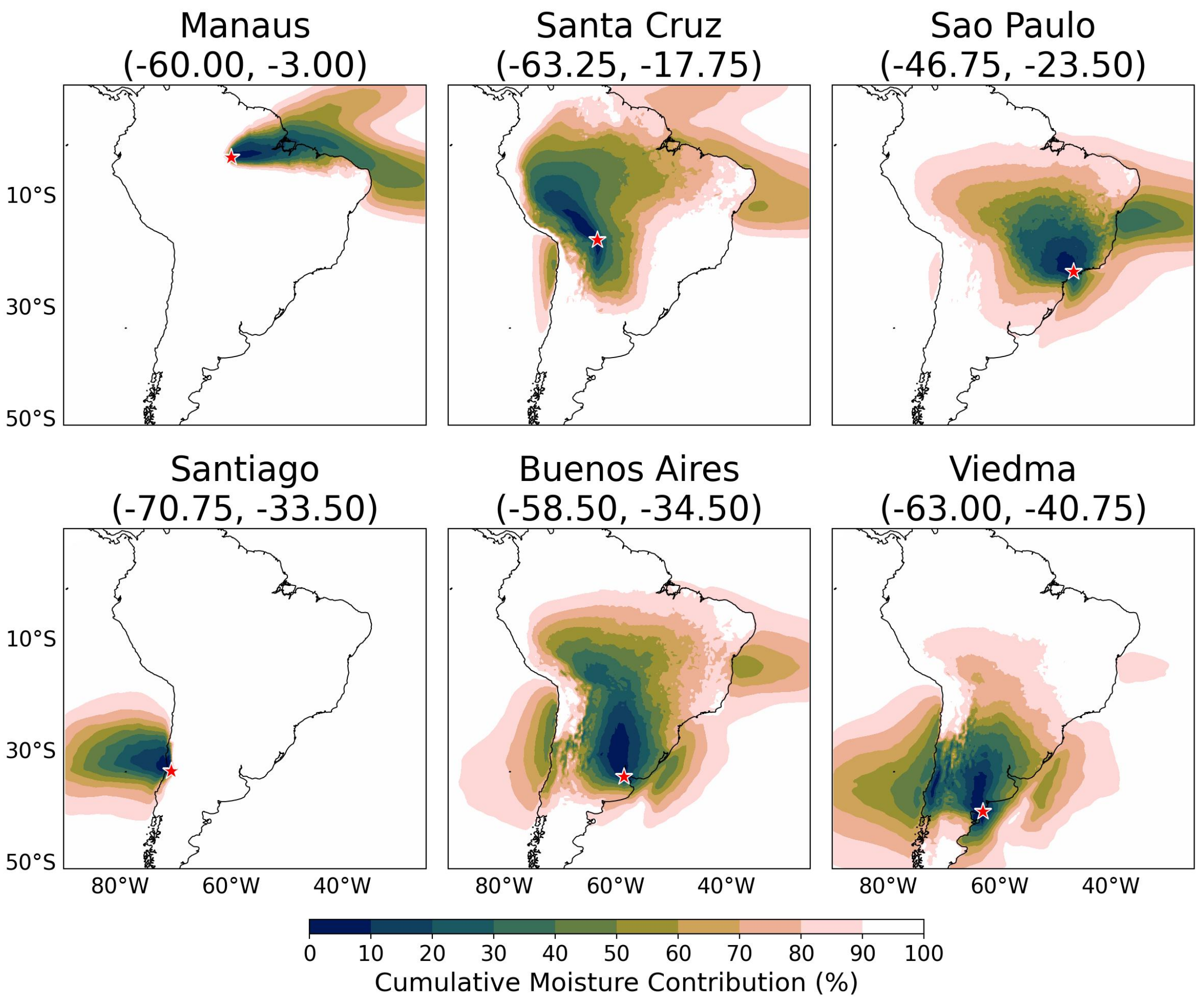

Figure 6. Thirty-year mean (1990–2019) precipitationsheds for six individually tagged 0.25° receptor cells (red stars): Manaus, Santa Cruz de la Sierra, and São Paulo (top row); Santiago, Buenos Aires, and Viedma (bottom row). Each panel is a per-panel spatial cumulative distribution of the tracked-evaporation source field (0% = the single strongest source cell; 100% = the diffuse tail), so that the dark core traces the region supplying most of each location's rainfall.

https://doi.org/10.5194/essd-2026-547
Preprint. Discussion started: 5 August 2026

moisture delivery to central-southern Chile (35°S–38°S) (Fig. 7). During the El Niño phase, enhanced subtropical moisture transport significantly increases the oceanic contribution to the austral winter and spring wet season — with box-mean tagged precipitation reaching 270 versus 68 mm month^{-1} in JJA — leading to markedly wetter winters (Poveda et al., 2001; Campos and Rondanelli, 2023). Conversely, the La Niña phase exhibits a stark reduction in moisture convergence, emphasising the dataset's utility in quantifying the spatial footprint of ENSO-driven water stress.

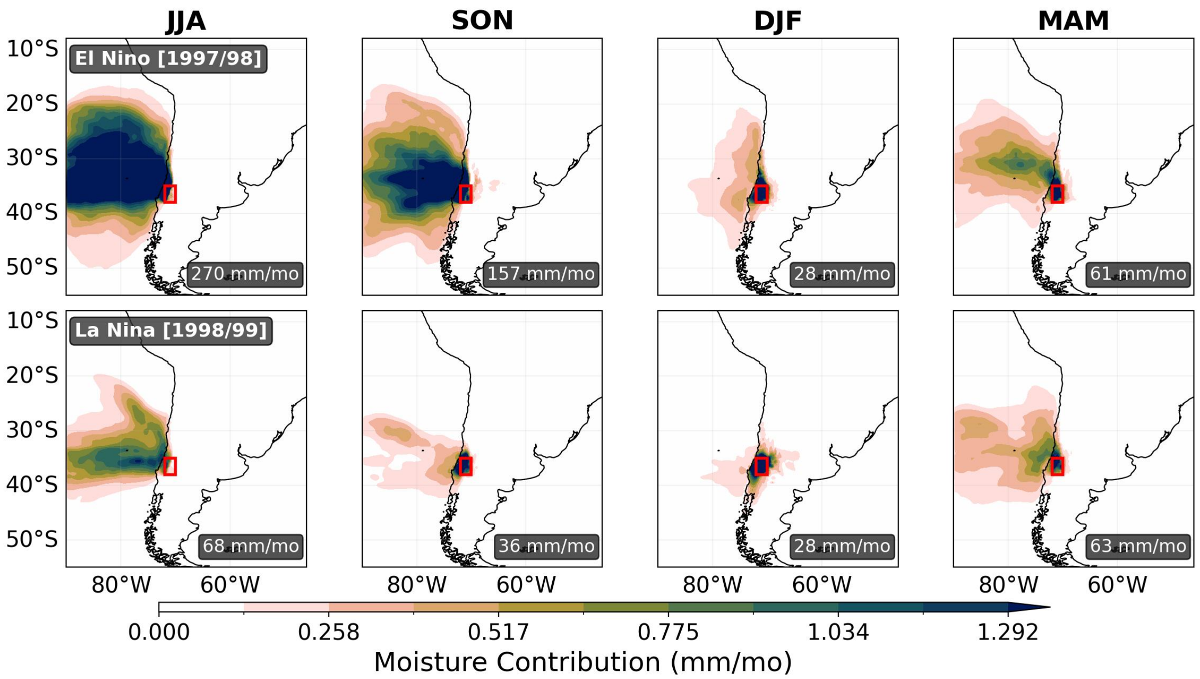

Figure 7. Seasonal evolution of moisture transport into central-south Chile (35°S–38°S; red box) through two contrasting ENSO events. Columns follow the ENSO life cycle (JJA, SON, DJF, MAM; DJF spans the year boundary): the top row composites the 1997/98 El Niño (JJA 1997 through MAM 1998) and the bottom row the subsequent 1998/99 La Niña (JJA 1998 through MAM 1999). Maps show the seasonal-mean tracked-evaporation source integrated over the receptor box; the value in the bottom-right corner of each panel is the area-weighted mean precipitation per grid cell (mm month^{-1}) within that box.

4.2 Democratising Big Data: ARCO and Lazy Loading

Traditionally, performing multi-decadal, high-resolution moisture tracking analyses required local access to massive storage arrays and High-Performance Computing (HPC) clusters. A major contribution of this work is the structural engineering of the dataset into an Analysis-Ready, Cloud-Optimized (ARCO) format. By hosting the compressed (∼8 TB) Zarr archive on a public cloud, we leverage the power of "lazy loading." Libraries such as Xarray allow users to virtually map the entire multi-terabyte dataset into their local Python environment without downloading the underlying arrays. Computations (such as temporal averaging or spatial subsetting) are deferred until the exact result is requested, at which point the code automatically

https://doi.org/10.5194/essd-2026-547
Preprint. Discussion started: 5 August 2026

downloads only the specific data chunks required for the analysis. Consequently, a researcher using a standard laptop with a basic internet connection can query 30 years of daily moisture flow data for a specific agricultural township in seconds. Paired with our open-source tutorial repositories, this infrastructure completely removes the computational barrier to entry.

4.3 Uncertainties and Limitations

While WAM2layers v3 provides highly efficient and mass-conserving Eulerian tracking, users must be aware of the inherent limitations associated with both the tracking algorithm and the atmospheric forcing data.

First, the accuracy of the tracking is entirely dependent on the quality of the underlying ERA5 reanalysis data. Reanalysis products do not perfectly close the terrestrial water budget; evaporation and precipitation are model-derived rather than directly assimilated from observations. Over topographically complex regions like the Andes or densely vegetated areas like the Amazon, ERA5 may struggle to accurately resolve localised convective precipitation or extreme topographic uplift, which may propagate into the moisture tracking results.

Second, Eulerian models fundamentally rely on the "well-mixed" assumption within their designated atmospheric layers. While the two-layer configuration of WAM2layers mitigates the vertical wind transport errors commonly found in older single-layer models, it remains an approximation of the highly complex, three-dimensional vertical mixing processes of the real atmosphere. Unlike Lagrangian trajectory models, Eulerian grid-based tracking cannot provide the exact, individual 3D path of an air parcel, but rather a statistical distribution of moisture fluxes across the grid boundaries. Furthermore, despite high-frequency temporal interpolation (10-min tracking timesteps), Eulerian models remain subject to minor numerical dispersion errors at the grid interfaces. Despite these limitations, the Eulerian approach remains a highly efficient and effective method for large-scale spatial analyses, but does not resolve the trajectory of any individual air parcel.

Third, because the tracking domain is spatially bounded, the exact geographic origin of moisture advected from far outside the South American continent cannot be explicitly resolved. While the Eulerian framework strictly closes the atmospheric water budget by recording moisture entering the tracking area as boundary fluxes (provided as `gains` in our dataset), it inherently truncates the far-field evaporative sources originating from the wider Pacific and Atlantic Oceans. Consequently, this product is exceptionally well-suited for identifying and analysing terrestrial moisture recycling and atmospheric transport within the continent itself. However, as emphasised by Kalverla et al. (2025), users must carefully consider the extent of the tracking domain. If a specific research question requires mapping the explicit spatial oceanic source origin for the vast majority (e.g., $> 80\%$) of a region's total precipitation, the aggregation of distant oceanic sources into domain boundary fluxes must be explicitly factored into the analysis.

4.4 Future Directions and Contributions to Open Science

The generation and publication of this dataset represent a significant step forward in hydroclimatology, serving not only as a regional resource but as a blueprint for future global atmospheric analyses. We highlight several broader impacts and future possibilities stemming from this work:

https://doi.org/10.5194/essd-2026-547
Preprint. Discussion started: 5 August 2026

– **A Pathway to a Global 0.25° Dataset:** By successfully parallelising and tracking ∼25,000 independent target grids across a continent as massive and climatologically complex as South America, we have proven the computational feasibility of ultra-high-resolution tracking. The methodologies and chunking strategies developed here provide a direct roadmap for expanding this effort into a seamless, global 0.25° moisture tracking dataset in the future.

– **Interdisciplinary Accessibility:** Because the ARCO architecture allows researchers to bypass the command-line intricacies of HPC systems, this dataset becomes highly accessible to interdisciplinary fields. Ecologists, agricultural scientists, and environmental policymakers with basic Python knowledge can now easily investigate how atmospheric moisture constraints impact forest resilience or crop yields, bridging the gap between atmospheric physics and applied environmental sciences.

5 Conclusions

In summary, this dataset represents an unprecedented leap in the scale, resolution, and accessibility of atmospheric moisture tracking data for South America. By providing a comprehensive 30-year record of daily moisture fluxes across ∼25,000 independent 0.25° grid cells, we deliver a foundational resource capable of capturing continental climatic shifts to highly localised eco-hydrological extremes.

Furthermore, by deploying this massive dataset via an Analysis-Ready, Cloud-Optimized architecture alongside comprehensive tutorials, we have effectively removed the steep computational barriers typically associated with moisture tracking. This empowers a much broader community of meteorologists, hydrologists, and ecologists to incorporate atmospheric water cycle dynamics into their research, directly advancing Earth system science in one of the planet's most critical regions.

6 Code and data availability

Dataset: The atmospheric moisture tracking dataset — an ∼8 TB Analysis-Ready, Cloud-Optimized (ARCO/Zarr) product derived from ∼230 TB of raw tracking output — is openly available on Hugging Face at https://doi.org/10.57967/hf/8650 (Hung and Lin, 2026), under the Creative Commons Attribution 4.0 licence. Calendar-month and calendar-year aggregates of the same dataset are provided at https://huggingface.co/datasets/AguaTrackSA/AguaTrack-ARCO-SA-Aggregated.

Code: The source code demonstrating how to query the cloud-optimised data and reproduce the analyses in this manuscript is openly available under the MIT License at github.com/NTU-CompHydroMet-Lab/AguaTrack-ARCO-SA-Tutorial, and archived on Zenodo at https://doi.org/10.5281/zenodo.20036507 (Lin and Hung, 2026).

Author contributions. HTH, KCT, WW, and LPW jointly conceived the ideas and conceptualised the research goals. HTH and SCL developed the methodology, implemented the software, curated the data, performed the formal analyses, and produced the visualisations.

https://doi.org/10.5194/essd-2026-547
Preprint. Discussion started: 5 August 2026

Open Access Earth System Science Data Discussions

HTH led the validation of the results and manuscript preparation. KCT, WW, and LPW were responsible for project supervision and funding acquisition. The authors thank Fu Ping for valuable discussions during the early stages of this study.

Competing interests. The contact author has declared that none of the authors has any competing interests.

Acknowledgements. All the figures used the colour palettes from Scientific colour maps (Crameri, 2023), distributed under the MIT License. The authors express their gratitude for the financial support from the National Science and Technology Council, Taiwan (grant NSTC 113-2923-M-002-001-MY4 to LPW and HTH; grants NSTC 113-2628-M-002-021- and 114-2628-M-002-014- to KCT) and the Ministry of Education, Taiwan (grant NTUJP-115L7215 to WW; grant NTU-114V1017-4 to KCT).

https://doi.org/10.5194/essd-2026-547
Preprint. Discussion started: 5 August 2026

Open Access Earth System Science Data Discussions

References

Ampuero, A., Stríkis, N. M., Apaéstegui, J., Vuille, M., Novello, V. F., Espinoza, J. C., Cruz, F. W., Vonhof, H., Mayta, V. C., Martins, V. T. S., Cordeiro, R. C., Azevedo, V., and Sifeddine, A.: The Forest Effects on the Isotopic Composition of Rainfall in the Northwestern Amazon Basin, Journal of Geophysical Research: Atmospheres, 125, e2019JD031 445, https://doi.org/10.1029/2019JD031445, 2020.

Arraut, J. M., Nobre, C., Barbosa, H. M. J., Obregon, G., and Marengo, J.: Aerial Rivers and Lakes: Looking at Large-Scale Moisture Transport and Its Relation to Amazonia and to Subtropical Rainfall in South America, Journal of Climate, 25, 543–556, https://doi.org/10.1175/2011JCLI4189.1, 2012.

Benedict, I., Van Heerwaarden, C. C., Van Der Ent, R. J., Weerts, A. H., and Hazeleger, W.: Decline in Terrestrial Moisture Sources of the Mississippi River Basin in a Future Climate, Journal of Hydrometeorology, 21, 299–316, https://doi.org/10.1175/JHM-D-19-0094.1, 2020.

Berger, M., Gerbens-Leenes, W., Karandish, F., Aldaya, M. M., Boulay, A.-M., Hogeboom, R. J., Link, A., Manzardo, A., Mialyk, O., Motoshita, M., Nuñez, M., Pfister, S., Rosenbaum, R. K., Scherer, L., Su, H., and Wöhler, L.: Complementary strengths of water footprint and life cycle assessments in analyzing global freshwater appropriation and its local impacts – Recommendations from an Interdisciplinary discussion series, Ecological Indicators, 174, 113 458, https://doi.org/10.1016/j.ecolind.2025.113458, 2025.

Boisier, J. P., Rondanelli, R., Garreaud, R. D., and Muñoz, F.: Anthropogenic and natural contributions to the Southeast Pacific precipitation decline and recent megadrought in central Chile, Geophysical Research Letters, 43, 413–421, https://doi.org/10.1002/2015GL067265, 2016.

Boisier, J. P., Alvarez-Garreton, C., Marinao, R., and Galleguillos, M.: Increasing water stress in Chile revealed by novel datasets of water availability, land use and water use, Hydrology and Earth System Sciences, 29, 5185–5212, https://doi.org/10.5194/hess-29-5185-2025, 2025.

Cai, W., McPhaden, M. J., Grimm, A. M., Rodrigues, R. R., Taschetto, A. S., Garreaud, R. D., Dewitte, B., Poveda, G., Ham, Y.-G., Santoso, A., Ng, B., Anderson, W., Wang, G., Geng, T., Jo, H.-S., Marengo, J. A., Alves, L. M., Osman, M., Li, S., Wu, L., Karamperidou, C., Takahashi, K., and Vera, C.: Climate impacts of the El Niño–Southern Oscillation on South America, Nature Reviews Earth & Environment, 1, 215–231, https://doi.org/10.1038/s43017-020-0040-3, 2020.

Campos, D. and Rondanelli, R.: ENSO-Related Precipitation Variability in Central Chile: The Role of Large Scale Moisture Transport, Journal of Geophysical Research: Atmospheres, 128, e2023JD038 671, https://doi.org/10.1029/2023JD038671, 2023.

Carvalho, L. M. V., Jones, C., and Liebmann, B.: The South Atlantic Convergence Zone: Intensity, Form, Persistence, and Relationships with Intraseasonal to Interannual Activity and Extreme Rainfall, Journal of Climate, 17, 88–108, https://doi.org/10.1175/1520-0442(2004)017<0088:TSACZI>2.0.CO;2, 2004.

Carver, R. W. and Merose, A.: ARCO-ERA5: An Analysis-Ready Cloud-Optimized Reanalysis Dataset, https://ams.confex.com/ams/103ANNUAL/meetingapp.cgi/Paper/415842, 2023.

Chen, J., Li, Y., Xiong, B., Wang, Y., Zhou, S., and Huang, Y.: Comparison of moisture sources of summer precipitation in 1998 and 2020 in the middle and lower reaches of Yangtze River basin, International Journal of Climatology, 43, 3493–3505, https://doi.org/10.1002/joc.8040, 2023.

Crameri, F.: Scientific colour maps, https://doi.org/10.5281/ZENODO.1243862, language: en, 2023.

Dirmeyer, P. A., Brubaker, K. L., and DelSole, T.: Import and export of atmospheric water vapor between nations, Journal of Hydrology, 365, 11–22, https://doi.org/10.1016/j.jhydrol.2008.11.016, 2009.

Eltahir, E. A. B. and Bras, R. L.: Precipitation recycling, Reviews of Geophysics, 34, 367–378, https://doi.org/10.1029/96RG01927, 1996.

Enciso, A. M., Baquero, O. L., Escobar-Carbonari, D., Tapasco, J., and Cerón, W. L.: Variability of Precipitation Recycling and Moisture Sources over the Colombian Pacific Region: A Precipitationshed Approach, Atmosphere, 13, 1202, https://doi.org/10.3390/atmos13081202, 2022.

Erfanian, A., Wang, G., and Fomenko, L.: Unprecedented drought over tropical South America in 2016: significantly under-predicted by tropical SST, Scientific Reports, 7, 5811, https://doi.org/10.1038/s41598-017-05373-2, 2017.

Espinoza Villar, J. C., Ronchail, J., Guyot, J. L., Cochonneau, G., Naziano, F., Lavado, W., De Oliveira, E., Pombosa, R., and Vauchel, P.: Spatio-temporal rainfall variability in the Amazon basin countries (Brazil, Peru, Bolivia, Colombia, and Ecuador), International Journal of Climatology, 29, 1574–1594, https://doi.org/10.1002/joc.1791, 2009.

Garreaud, R., Boisier, J. P., Alvarez-Garreton, C., Christie, D. A., Carrasco-Escaff, T., Vergara, I., Chávez, R. O., Alduncе, P., Camus, P., Suazo-Álvarez, M., Masiokas, M., Castro, G., Muñoz, A., Zambrano-Bigiarini, M., Fuster, R., and Godoy, L.: Hyperdroughts in central Chile: drivers, impacts, and projections, Hydrology and Earth System Sciences, 29, 5347–5369, https://doi.org/10.5194/hess-29-5347-2025, 2025.

Garreaud, R. D.: The Andes climate and weather, Advances in Geosciences, 22, 3–11, https://doi.org/10.5194/adgeo-22-3-2009, 2009.

Garreaud, R. D., Alvarez-Garreton, C., Barichivich, J., Boisier, J. P., Christie, D., Galleguillos, M., LeQuesne, C., McPhee, J., and Zambrano-Bigiarini, M.: The 2010–2015 megadrought in central Chile: impacts on regional hydroclimate and vegetation, Hydrology and Earth System Sciences, 21, 6307–6327, https://doi.org/10.5194/hess-21-6307-2017, 2017.

Guo, L., Van Der Ent, R. J., Klingaman, N. P., Demory, M.-E., Vidale, P. L., Turner, A. G., Stephan, C. C., and Chevuturi, A.: Moisture Sources for East Asian Precipitation: Mean Seasonal Cycle and Interannual Variability, Journal of Hydrometeorology, 20, 657–672, https://doi.org/10.1175/JHM-D-18-0188.1, 2019.

Hersbach, H., Bell, B., Berrisford, P., Hirahara, S., Horányi, A., Muñoz-Sabater, J., Nicolas, J., Peubey, C., Radu, R., Schepers, D., Simmons, A., Soci, C., Abdalla, S., Abellan, X., Balsamo, G., Bechtold, P., Biavati, G., Bidlot, J., Bonavita, M., De Chiara, G., Dahlgren, P., Dee, D., Diamantakis, M., Dragani, R., Flemming, J., Forbes, R., Fuentes, M., Geer, A., Haimberger, L., Healy, S., Hogan, R. J., Hólm, E., Janisková, M., Keeley, S., Laloyaux, P., Lopez, P., Lupu, C., Radnoti, G., De Rosnay, P., Rozum, I., Vamborg, F., Villaume, S., and Thépaut, J.: The ERA5 global reanalysis, Quarterly Journal of the Royal Meteorological Society, 146, 1999–2049, https://doi.org/10.1002/qj.3803, 2020.

Hung, H. T. and Lin, S. C.: AguaTrack-ARCO-SA (Revision a433c0f), https://doi.org/10.57967/hf/8650, 2026.

Kalverla, P., Benedict, I., Weijenborg, C., and Van Der Ent, R. J.: Atmospheric moisture tracking with WAM2layers v3, Geoscientific Model Development, 18, 4335–4352, https://doi.org/10.5194/gmd-18-4335-2025, 2025.

Keys, P. W., Van Der Ent, R. J., Gordon, L. J., Hoff, H., Nikoli, R., and Savenije, H. H. G.: Analyzing precipitationsheds to understand the vulnerability of rainfall dependent regions, Biogeosciences, 9, 733–746, https://doi.org/10.5194/bg-9-733-2012, 2012.

Keys, P. W., Barnes, E. A., Van Der Ent, R. J., and Gordon, L. J.: Variability of moisture recycling using a precipitationshed framework, Hydrology and Earth System Sciences, 18, 3937–3950, https://doi.org/10.5194/hess-18-3937-2014, 2014.

Keys, P. W., Wang-Erlandsson, L., and Gordon, L. J.: Megacity precipitationsheds reveal tele-connected water security challenges, PLOS ONE, 13, e0194 311, https://doi.org/10.1371/journal.pone.0194311, 2018.

Keys, P. W., Collins, P. M., Chaplin-Kramer, R., and Wang-Erlandsson, L.: Atmospheric water recycling an essential feature of critical natural asset stewardship, Global Sustainability, 7, e2, https://doi.org/10.1017/sus.2023.24, 2024.

https://doi.org/10.5194/essd-2026-547
Preprint. Discussion started: 5 August 2026

Li, Y., Wang, C., Tang, Q., Yao, S., Sun, B., Peng, H., and Xiao, S.: Unraveling the discrepancies between Eulerian and Lagrangian moisture tracking models in monsoon- and westerly-dominated basins of the Tibetan Plateau, Atmospheric Chemistry and Physics, 24, 10 741–10 758, https://doi.org/10.5194/acp-24-10741-2024, 2024.

Lin, S. C. and Hung, H. T.: AguaTrack-ARCO-SA Tutorial, https://doi.org/10.5281/zenodo.20036507, 2026.

Link, A., Van Der Ent, R., Berger, M., Eisner, S., and Finkbeiner, M.: The fate of land evaporation – a global dataset, Earth System Science Data, 12, 1897–1912, https://doi.org/10.5194/essd-12-1897-2020, 2020.

Lobos-Roco, F., Hartogensis, O., Suárez, F., Huerta-Viso, A., Benedict, I., De La Fuente, A., and Vilà-Guerau De Arellano, J.: Multi-scale temporal analysis of evaporation on a saline lake in the Atacama Desert, Hydrology and Earth System Sciences, 26, 3709–3729, https://doi.org/10.5194/hess-26-3709-2022, 2022.

Magrin, G. O., Marengo, J. A., Boulanger, J.-P., Buckeridge, M. S., Castellanos, E., Poveda, G., Scarano, F. R., and Vicuña, S.: Central and South America, in: Climate Change 2014: Impacts, Adaptation, and Vulnerability. Part B: Regional Aspects. Contribution of Working Group II to the Fifth Assessment Report of the Intergovernmental Panel on Climate Change, edited by Barros, V. R., Field, C. B., Dokken, D. J., Mastrandrea, M. D., Mach, K. J., Bilir, T. E., Chatterjee, M., Ebi, K. L., Estrada, Y. O., Genova, R. C., Girma, B., Kissel, E. S., Levy, A. N., MacCracken, S., Mastrandrea, P. R., and White, L. L., pp. 1499–1566, Cambridge University Press, Cambridge, United Kingdom and New York, NY, USA, https://hdl.handle.net/10669/89608, 2014.

Marengo, J. A., Soares, W. R., Saulo, C., and Nicolini, M.: Climatology of the Low-Level Jet East of the Andes as Derived from the NCEP–NCAR Reanalyses: Characteristics and Temporal Variability, Journal of Climate, 17, 2261–2280, https://doi.org/10.1175/1520-0442(2004)017<2261:COTLJE>2.0.CO;2, 2004.

Montecinos, A. and Aceituno, P.: Seasonality of the ENSO-Related Rainfall Variability in Central Chile and Associated Circulation Anomalies, Journal of Climate, 16, 281–296, https://doi.org/10.1175/1520-0442(2003)016<0281:SOTERR>2.0.CO;2, 2003.

Mu, Y., Biggs, T. W., and De Sales, F.: Forests Mitigate Drought in an Agricultural Region of the Brazilian Amazon: Atmospheric Moisture Tracking to Identify Critical Source Areas, Geophysical Research Letters, 48, e2020GL091 380, https://doi.org/10.1029/2020GL091380, 2021.

Mu, Y., Biggs, T. W., and Jones, C.: Importance in Shifting Circulation Patterns for Dry Season Moisture Sources in the Brazilian Amazon, Geophysical Research Letters, 50, e2023GL103 167, https://doi.org/10.1029/2023GL103167, 2023.

Posada-Marín, J., Salazar, J., Rulli, M. C., Wang-Erlandsson, L., and Jaramillo, F.: Upwind moisture supply increases risk to water security, Nature Water, 2, 875–888, https://doi.org/10.1038/s44221-024-00291-w, 2024.

Poveda, G., Jaramillo, A., Gil, M. M., Quiceno, N., and Mantilla, R. I.: Seasonally in ENSO-related precipitation, river discharges, soil moisture, and vegetation index in Colombia, Water Resources Research, 37, 2169–2178, https://doi.org/10.1029/2000WR900395, 2001.

Salio, P., Nicolini, M., and Zipser, E. J.: Mesoscale Convective Systems over Southeastern South America and Their Relationship with the South American Low-Level Jet, Monthly Weather Review, 135, 1290–1309, https://doi.org/10.1175/MWR3305.1, 2007.

Seluchi, M. E., Chan Chou, S., and Gramani, M.: A case study of a winter heavy rainfall event over the Serra do Mar in Brazil, Geofísica Internacional, 50, https://doi.org/10.22201/igeof.00167169p.2011.50.1.121, 2011.

Seneviratne, S. I., Lüthi, D., Litschi, M., and Schär, C.: Land–atmosphere coupling and climate change in Europe, Nature, 443, 205–209, https://doi.org/10.1038/nature05095, 2006.

Shi, K., Li, T., Zhao, J., Su, Y., Gao, J., and Li, J.: Atmospheric recycling of agricultural evapotranspiration in the Tarim Basin, Frontiers in Earth Science, 10, 950 299, https://doi.org/10.3389/feart.2022.950299, 2022.

Tian, B., Wu, W., Yang, Z., and Zhou, Y.: Drivers, trends, and potential impacts of long-term coastal reclamation in China from 1985 to 2010, ESTUARINE COASTAL AND SHELF SCIENCE, 170, 83–90, https://doi.org/10.1016/j.ecss.2016.01.006, num Pages: 8 Place: London Web of Science ID: WOS:000372379900008 remark: 1985 - 2010 # China's coastline across nine coastal provinces and two metropolises # Landsat imagery, remote sensing and geographic information systems., 2016.

Tuinenburg, O. A. and Staal, A.: Tracking the global flows of atmospheric moisture and associated uncertainties, Hydrology and Earth System Sciences, 24, 2419–2435, https://doi.org/10.5194/hess-24-2419-2020, 2020.

Tuinenburg, O. A., Theeuwen, J. J. E., and Staal, A.: High-resolution global atmospheric moisture connections from evaporation to precipitation, Earth System Science Data, 12, 3177–3188, https://doi.org/10.5194/essd-12-3177-2020, 2020.

Van Der Ent, R. J. and Tuinenburg, O. A.: The residence time of water in the atmosphere revisited, Hydrology and Earth System Sciences, 21, 779–790, https://doi.org/10.5194/hess-21-779-2017, 2017.

Van Der Ent, R. J., Savenije, H. H. G., Schaefli, B., and Steele-Dunne, S. C.: Origin and fate of atmospheric moisture over continents, Water Resources Research, 46, 2010WR009 127, https://doi.org/10.1029/2010WR009127, 2010.

Van Der Ent, R. J., Wang-Erlandsson, L., Keys, P. W., and Savenije, H. H. G.: Contrasting roles of interception and transpiration in the hydrological cycle – Part 2: Moisture recycling, Earth System Dynamics, 5, 471–489, https://doi.org/10.5194/esd-5-471-2014, 2014.

Wang-Erlandsson, L., Fetzer, I., Keys, P. W., Van Der Ent, R. J., Savenije, H. H. G., and Gordon, L. J.: Remote land use impacts on river flows through atmospheric teleconnections, Hydrology and Earth System Sciences, 22, 4311–4328, https://doi.org/10.5194/hess-22-4311-2018, 2018.

Weng, W., Luedeke, M. K. B., Zemp, D. C., Lakes, T., and Kropp, J. P.: Aerial and surface rivers: downwind impacts on water availability from land use changes in Amazonia, Hydrology and Earth System Sciences, 22, 911–927, https://doi.org/10.5194/hess-22-911-2018, 2018.

Weng, W., Costa, L., Lüdeke, M. K., and Zemp, D. C.: Aerial river management by smart cross-border reforestation, Land Use Policy, 84, 105–113, https://doi.org/10.1016/j.landusepol.2019.03.010, 2019.

Weng, W., Becker, S. L., Lüdeke, M. K., and Lakes, T.: Landscape matters: Insights from the impact of mega-droughts on Colombia's energy transition, Environmental Innovation and Societal Transitions, 36, 1–16, https://doi.org/10.1016/j.eist.2020.04.003, 2020.

Zan, B., Ge, J., Mu, M., Sun, Q., Luo, X., and Wei, J.: Spatiotemporal inequality in land water availability amplified by global tree restoration, Nature Water, 2, 863–874, https://doi.org/10.1038/s44221-024-00296-5, 2024.

Zemp, D. C., Schleussner, C.-F., Barbosa, H. M. J., Van Der Ent, R. J., Donges, J. F., Heinke, J., Sampaio, G., and Rammig, A.: On the importance of cascading moisture recycling in South America, Atmospheric Chemistry and Physics, 14, 13 337–13 359, https://doi.org/10.5194/acp-14-13337-2014, 2014.

Zemp, D. C., Schleussner, C.-F., Barbosa, H. M. J., Hirota, M., Montade, V., Sampaio, G., Staal, A., Wang-Erlandsson, L., and Rammig, A.: Self-amplified Amazon forest loss due to vegetation-atmosphere feedbacks, Nature Communications, 8, 14 681, https://doi.org/10.1038/ncomms14681, 2017.

Zhang, B., He, Y., Ren, Y., Huang, B., Peng, Y., Wang, S., and Guan, X.: The influence of the precipitation recycling process on the shift to heavy precipitation over the Tibetan Plateau in the summer, Frontiers in Earth Science, 11, 1078 501, https://doi.org/10.3389/feart.2023.1078501, 2023.

Zhang, C.: Moisture sources for precipitation in Southwest China in summer and the changes during the extreme droughts of 2006 and 2011, Journal of Hydrology, 591, 125 333, https://doi.org/10.1016/j.jhydrol.2020.125333, 2020.